Solvent-free production of thermoplastic lignocellulose from wood pulp by reactive extrusion

Jinlei Li[a], Thomas Baker[a], Guerino G. Sacripante[a], David Lawton[b], Heera Marway[a], Hongfeng Zhang[a], Michael Thompson[a,*]

[a] *Department of Chemical Engineering, McMaster University, Hamilton, ON L8S 4L8, Canada*

[b] *Xerox Research Centre of Canada, Mississauga, ON L5K 2L1, Canada*

* Corresponding author at: Department of Chemical Engineering, McMaster University, Hamilton, ON L8S 4L8, Canada.

E-mail address: mthomps@mcmaster.ca (M. Thompson).

ABSTRACT

A novel acylation approach suited to rapid bulk thermoplasticization of lignocellulose without solvents was previously demonstrated by the authors in benchtop batch studies. The method relies upon a benzethonium chloride/sulfuric acid functionalizing agent at low concentrations to act as a wetting agent for the wood pulp, similar to an ionic liquid, yet binds to the lignocellulose ester as a flow aid in the final thermoplastic. The present investigation evaluates the approach in a residence time-limited (45-90 s) continuous twin-screw reactor, where intensive mixing and heat were found to yield high acylation. The modified lignocellulose exhibited desired thermoplasticity by being melt moldable without the need for plasticizers and maintained much of the excellent stiffness of cellulose, demonstrating a maximum flexural modulus of 5.4 GPa and tensile modulus of 1.8 GPa. The influence of extrusion conditions on thermoplasticity was examined by a Design of Experiments (DOE) analysis.

Keywords: Lignocellulose; Thermoplasticization; Mechanochemistry; Reactive extrusion.

1. INTRODUCTION

Lignocellulose is a renewable, abundant and structurally strong biopolymer, considered to be an attractive alternative to current plastics due to declining fossil fuel reserves. This complex polymeric system is composed of cellulose, hemicellulose and lignin, and due to strong intra- and inter interactions among the present species, it lacks flowable properties attributed to thermoplastics. The absence of melt-like behavior, right up to its decomposition temperature, renders this native biomass unusable in conventional and economical polymer processing methods. Chemical modifications of the hydroxyl groups within the components of lignocellulose can interfere with hydrogen bonding and introduce side groups, which beneficially improves chain mobility to yield thermoplasticity as a result (Abe, Enomoto, Seki, & Miki, 2020; Bao et al., 2018; Chen et al., 2017; Chen & Shi, 2015; Feng et al., 2019; Guo, Chen, Su, & Hong, 2018; Xie, King, Kilpelainen, Granstrom, & Argyropoulos, 2007). The challenge for modifying lignocellulose is the lack of adequate available solvents to wet and dissolve its fibrillar structure, both quickly and extensively, such that enough hydroxyl functional groups are made chemically available for reactions. Innovative modification methods in the literature have recently focused on ionic liquids and their cosolvents (Chen et al., 2017; Chen & Shi, 2015; Guo et al., 2018; Xie et al., 2007) due to the improved chemical site accessibility found for reactions. Despite their effectiveness, an excess amount of these solvents has been reportedly needed, and due to the high expense of these chemicals, there must be costly recovery techniques deployed after a modification.

Mechanochemistry, using mechanical energy to induce and assist reactions, can eliminate or dramatically reduce the solvent need for reactions (Darwish, Wang, Croker, Walker, & Zaworotko, 2019; Howard, Cao, & Browne, 2018). Mechanical techniques like milling or grinding can effectively defibrillate lignocellulose (Correia et al., 2016; Espinosa, Rol, Bras, & Rodríguez,

2019; Hoeger et al., 2013; Jiang, Wang, Zhang, & Wolcott, 2017). The defibrillation of lignocellulose is another beneficial means, like good solvents, for improving the accessibility of its hydroxyl groups for reactions (Huang, Wu, Wang, & Wolcott, 2019; Li, Thompson, & Lawton, 2019; Ochiai et al., 2019). Thereby, mechanochemical modification, mainly by ball milling, has been demonstrated to be an effective method to functionalize fibrillar biomass without pre-dissolving these fibrils, as a consequence, significantly reducing the amount of liquids required for the chemical modifications (Chen et al., 2019; Gan et al., 2018; Huang, Wu, Wang, Ou, & Wolcott, 2020; Zhang et al., 2018). However, milling has problems with temperature control and usually needs long treatment times, especially when a high degree of modification is sought. Twin-screw extruders are designed to operate at elevated temperature with precise control and generate very high, localized mechanical stresses, making them more suitable for mechanochemistry than mills, especially if reaction rates can be matched to the short residence time of the process. Twin-screw extrusion has recently been demonstrated to be more effective in defibrillating lignocellulose or cellulose than milling (Baati, Mabrouk, Magnin, & Boufi, 2018; Baati, Magnin, & Boufi, 2017; Espinosa et al., 2019; Ho, Abe, Zimmermann, & Yano, 2015; Rol et al., 2017). Therefore, reactive extrusion has been explored for functionalizing lignocellulose or cellulose due to its suitable thermo-mechanical environment and because continuous systems like extrusion tend to offer higher quality consistency under more economical conditions compared to batch systems (Bhandari, Jones, & Hanna, 2012; Vaidya, Gaugler, & Smith, 2016; Zhang, Li, Li, Gibril, & Yu, 2014). Due to challenges with the short residence time of the extruder and difficulties with conveying non-viscous lignocellulose, to our knowledge, this study is the first to modify lignocellulose into a flowable thermoplastic by reactive extrusion.

A previous paper (Li et al., 2020) introducing the modification approach used in the present study showed the effectiveness of the chemistry in a batch system but not whether it was scalable to a continuous method like extrusion. The benchtop batch method effectively modified lignocellulosic wood pulp into a thermoplastic with good flowability, demonstrated by compression molding, but in that case, lengthy reaction times were used to maximize conversion. The current work examines the benefits of mechanochemistry in order to produce comparable thermoplastics from the lignocellulose within the dramatically shorter residence time of a twin-screw extruder. The influence of extrusion conditions with two different acid anhydrides is studied on the thermoplasticity and physical properties of the modified lignocellulose.

2. Materials and methods

2.1. Materials

Lignocellulosic wood pulp containing 8.2 wt% Klason lignin (determined by TAPPI-T method 222 om-02) was received from Tembec (Montreal, Canada) as a high-yield Aspen mechanical pulp. The received pulp was pulverized in a 27 mm 40 L/D corotating twin-screw extruder (Leistritz, USA) according to a previously established method (Li et al., 2019). By this method, the received fluffy wood pulp was converted into granules with an improved degree of fibrillation, which made it convenient for feeding into the process for reactions and improved its chemical accessibility. Benzethonium chloride (hyamine, HPLC grade), sodium bicarbonate and phenolphthalein (ACS grade), and butyric anhydride (reagent grade) were purchased from Sigma Aldrich (Oakville, Canada). Acetic anhydride (reagent grade), sulfuric acid (trace metal grade), dimethyl sulfoxide (DMSO) and anhydrous ethanol (reagent grade), and 1.0 M sodium hydroxide and hydrochloric acid solutions were obtained from Caledon Laboratory Ltd. (Georgetown, Canada).

2.2. Chemical modification of lignocellulosic wood pulp by reactive extrusion

Reactive extrusion of the pulverized lignocellulosic pulp was done by an 18 mm 40 L/D corotating twin-screw extruder (Leistritz, USA), as shown in Scheme 1. The screw configuration contained one 30° offset kneading block early in the process to aid wetting by further defibrillation of the pulp, followed by four 90° offset kneading blocks in a row later to supply sufficient mixing for the modification. The delayed input of substantial mechanical stresses was prudent to avoid jamming the extruder, relying on swollen and partially modified lignocellulose to lubricate the zone of most intensive mechanochemistry. Air-dried pulverized pulp was fed by a gravimetric feeder (Coperion, Germany) at a rate of 500 g/h. The feed zone temperature was maintained at 25 °C by chilled water, while the other zones were all heated. Table 1 presents the series of experiments that were conducted based on a DOE method. The extrusion temperature for the butyric anhydride series (BA-series) (Table 1a) was set to 120 or 140 °C, but only 120 °C for the acetic anhydride series (AA-series) (Table 1b). The liquid modifier was injected into the second zone with an Optos Series metering pump (Eldex, USA) at a rate of 32 or 48 mL/min that corresponded to a 3.8 and 5.8 liquid/lignocellulose ratio, respectively. The liquid modifier (reactant and functionalizing agent) was pre-made by dissolving 30 g hyamine per 100 mL anhydride under constant agitation at 120 °C, and then adding sulfuric acid dropwise to the solution until the molar ratio of sulfuric acid/hyamine was either 0.95 or 1.20, according to our previously estimated procedure (Li et al., 2020). The acidic liquid modifier produced no detectable corrosion in the twin-screw extruder at these molar ratios, making the chemistry suitable for manufacturing. The screw speed of the extruder was set to either 100 rpm or 300 rpm based on the chosen experimental conditions (Table 1). The DOE presented in Table 1 was set up and analyzed using SigmaXL software (SigmaXL Inc., Kitchener, Canada).

The modified lignocellulose exiting from the extruder was collected, cooled and then suspended in distilled water for cleaning. Cleaning was necessary due to the far-from-optimized chemistry presented in this first study on the modification. The suspended material was neutralized with 1M sodium bicarbonate solution, filtered and then repeatedly washed with distilled water until the conductivity of the filtrate was close to that of distilled water (determined by a Mettler Toledo S230 conductivity meter). A cleaned sample was vacuum-oven dried at 75 °C for 24 hours prior to storage and characterization.

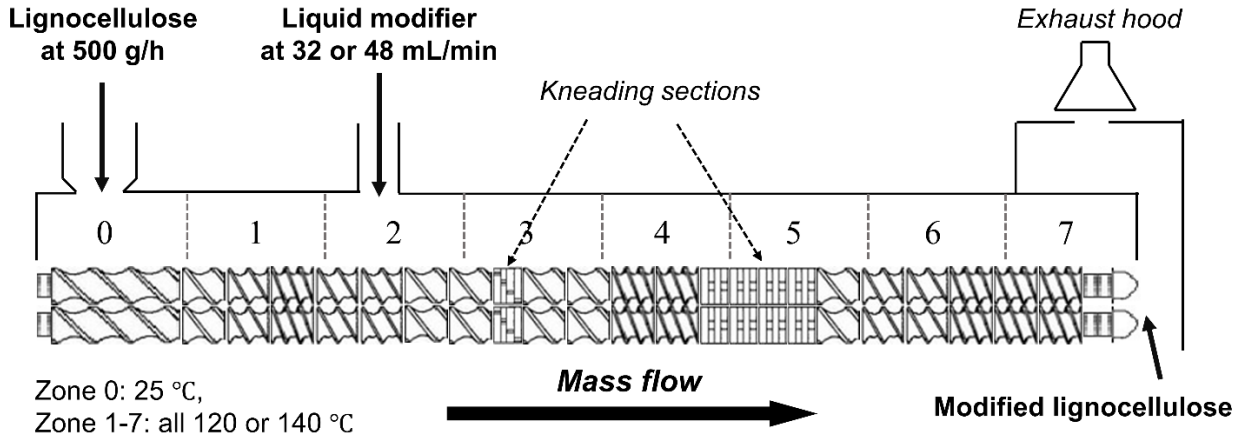

Scheme 1. Configuration of the extruder used for modification of lignocellulosic wood pulp.

Table 1: DOE layout for studying the effects of extrusion conditions on the chemical modifications of lignocellulose, (a) BA-series using butyric anhydride and (b) AA-series using acetic anhydride.

(a)

Run No.	Liquid injection rate (mL/min)	Screw speed (rpm)	Molar (sulfuric acid/hyamine)	Temperature (°C)
	A	**B**	**C**	**D**
B1	32	100	0.95	120
B2	32	300	1.20	120
B3	32	100	1.20	140
B4	32	300	0.95	140
B5	48	100	1.20	120
B6	48	300	0.95	120
B7	48	100	0.95	140
B8	48	300	1.20	140

(b)

Run No.	Liquid injection rate (mL/min)	Screw speed (rpm)	Molar (sulfuric acid/hyamine)
	A	**B**	**C**
A1	32	100	0.95
A2	32	100	1.20
A3	32	300	0.95
A4	32	300	1.20
A5	48	100	0.95
A6	48	100	1.20
A7	48	300	0.950
A8	48	300	1.20

2.3. Compression molding of the modified lignocellulose

Specimens with different dimensions (D1: 50 mm × 50 mm × 0.26 mm; D2: 50 mm × 13 mm × 0.45 mm; D3: 55 mm × 15 mm × 2 mm) were compression molded to test the thermal moldability of the modified lignocellulose. Molding was done in a Carver 4389 benchtop hydraulic press under 2.5 MPa for 3 mins and then 6 MPa for another 12 mins. Molding temperatures for BA-series and AA-series were 150 and 180 °C, respectively.

2.4. Characterizations

2.4.1. Minimum residence time

The minimum residence time of the twin-screw extrusion was measured by using a carbon black tracer. The carbon black was introduced as a pulse into the feed zone along with the lignocellulose and timed until it first appeared at the exit. This characterization represents the minimum time allowed for the reaction.

2.4.2. Chemical structures

Infrared spectra (FTIR) were collected on a Nicolet 6700 spectrometer with a Smart iTRTM attenuated total reflectance (ATR) sampling accessory. A spectrum was generated from 32 scans in the range of 4000-500 cm^{-1} with a 4 cm^{-1} resolution. Solution state ^{13}C nuclear magnetic resonance (NMR) spectroscopy of modified samples was performed in DMSO-d6 solvent with a Bruker AVIII 700 MHz spectrometer at ambient temperature. The NMR spectra were obtained from 2560 scans with a 600 MHz magnetic field, 4 s of relaxation time and 1 s of retention time for the ^{13}C nuclei.

Acyl and benzethonium sulfate contents of the modified lignocellulose were determined by colorimetric titration and elemental analysis (Supporting Information). Dried modified

lignocellulose, 0.05 g, was put into a 25-mL glass vial, to which was added 5 mL of 0.25 M NaOH and 5 mL of anhydrous ethanol. The mixture was left to stand for 24 h before 10 mL of 0.25 M HCl was added to the system. After 30 mins, the mixture was titrated by 0.25 M NaOH with a phenolphthalein indicator. The total hydrolyzed ester content (TEC) was calculated by:

$$TEC\ \left(\frac{mmol}{g}\right) = \frac{(V_1+V_2)C_1-V_3C_2}{m} \quad (1)$$

where V_1 (mL) is the volume of NaOH added to the system before the titration, V_2 (mL) is the volume of NaOH consumed in the titration, C_1 (M) is the NaOH concentration, V_3 (mL) is the volume of HCl added to the system before the titration, C_2 (M) is the concentration of HCl, and m is the weight of the sample.

Elemental nitrogen (N) and sulfur (S) contents were determined with a UNICUBE elemental analyzer (Elementar). Approximately 2 mg powder sample was sealed in Tinfoil and loaded into the analyzer for testing.

Inherent and intrinsic viscosity were used to assess the degradation for the modified lignocellulose samples with a Cannon Fenske viscometer (25-tube size). 40 mg dried sample was added to 40 mL DMSO solvent and stirring overnight to dissolve the lignocellulose; the insoluble part was separated by filtering and dried to determine the concentration (c) of the solution. The neat solvent or modified lignocellulose solution flowed through the viscometer held at 25 °C, and their flow times through the graduated region were recorded. Inherent viscosity (η_{inh}) was determined from the flow times of the DMSO solvent(t_0) and solution of the modified lignocellulose (t), according to:

$$\eta_{inh} = \mathrm{In}\left(\frac{t}{t_0}/c\right) \quad (2)$$

Intrinsic viscosity was estimated as the intercept of inherent viscosity curves versus concentration.

2.4.3. Thermal properties

Thermal transitions were determined by dynamic mechanical analysis (DMA) and differential scanning calorimetry (DSC). DMA testing was performed on an 850 analyzer (TA Instruments, USA). The measurements were performed in a tension model on rectangular specimens with a dimension of 30 mm × 5 mm × 0.45 mm cut from the compression-molded samples. The scanning was performed at a frequency of 1 Hz and a strain of 0.01%, with temperature ramping from 10-240 ℃ by 3 ℃/min. DSC testing was accomplished by a Q200 calorimeter (TA Instruments, USA) operating in modulated mode. Modified pulp, 9 mg, was loaded and sealed into a Tzero aluminum pan. Samples were equilibrated at -20 ˚C, then heated to 220 ˚C at the ramp rate of 5 ˚C/min, with an oscillation of 1.00 ˚C every 60 seconds.

Thermo-flowability was quantified with a Discovery HR-2 hybrid rheometer (TA Instruments, USA) by conducting a temperature sweep after first discovering the linear response region by a strain sweep. A circular disk with 1.50 mm thickness and 25 mm diameter was prepared by compression molding for the rheology testing. The testing was performed in an ambient atmosphere by sweeping temperature from 90 to 200 ˚C at a rate of 5 ˚C/min, and under a constant shear rate of 0.1 s^{-1}.

2.4.4. Mechanical properties

Tensile and 3-point flexural properties were measured on strips with a dimension of 50 mm × 13 mm × 0.45 mm by an Instron universal mechanical tester (Model 3366). The tensile testing was performed at a crosshead speed of 0.085 mm/min by following standard ASTM D882-18, and force was recorded with a 0.5 kN load cell. The 3-point flexural testing was conducted at a crosshead speed of 2.5 mm/min by standard ASTM D790, and the force was recorded with a 0.05 kN load cell. The length of the support span for the flexural testing was 26 mm. Mechanical properties were reported as the average of three repeats.

206 *2.4.5. Morphology property*

207 The cross-sections of mold specimens after bending were observed by scanning electron
208 microscopy (SEM) with a SU8000 FE-SEM (Hitachi, Japan) operating at 5 kV. In preparation,
209 samples were sputter coated with a 6 nm thick layer of Pt/Pd before observation.

210 **3. RESULTS AND DISCUSSION**

211 *3.1. Chemical structure of the modified lignocellulose*

212 The FTIR spectra (Fig. S1) indicated that compared to the original material, the modified
213 lignocellulose presented a strong peak at 1740 cm^{-1} corresponding to ester species (-COO-) (Zhen
214 et al., 2016). Correspondingly, there was a considerable decrease in the hydroxyl functionality of
215 lignocellulose, based on the decreasing intensity of the broad peak centered at 3330 cm^{-1}. A sulfate
216 functionality was detected in the modified lignocellulose at 837 cm^{-1} (-C-O-S- symmetrical
217 vibration) and 602 cm^{-1} (bending mode of sulfate) (Böke, Akkurt, Özdemir, Göktürk, & Caner
218 Saltik, 2004; Chen, Zhang, Zhao, & Chen, 2013). According to previous batch studies, the sulfate
219 species were formed by reaction between hydroxyl groups and sulfuric acid or bisulfate in the
220 liquid modifier (Li et al., 2020).

221 Fig. 1 shows solution-state ^{13}C NMR spectra of the modified lignocellulose produced by
222 reactive extrusion using acetic and butyric anhydride. Labelled with solid arrows in the plot (a),
223 the chemical shifts at 170-174 ppm of the modified lignocellulose in the BA-series were assigned
224 to the butyryl carbonyl group; three shifts at 13, 18 and 35 ppm corresponded to the three carbons
225 of butyryl (Huang et al., 2011; Zhang et al., 2018). Similarly, for the AA-series in the plot (b),
226 shifts at 169-171 ppm and 21 ppm were assigned to carbonyl and methyl carbons of the acetyl
227 functionality, respectively (Kono, Oka, Kishimoto, & Fujita, 2017; Ralph & Landucci, 2010).
228 Despite the short reaction time in the extruder, both reactions with the acid anhydrides forming

lignocellulose esters were significant; the minimum residence time inside the extruder was 90 or 45 s, respectively, when a screw speed of 100 or 300 rpm was used. Additionally, the NMR result shows that the modified lignocellulose also included similar chemical shifts to hyamine (plot (c)), as highlighted with rectangular symbols, which were assigned to the benzethonium cation of hyamine. The attached cation could not be clearly observed by FTIR due to its weaker signal and interfering peaks by lignocellulose.

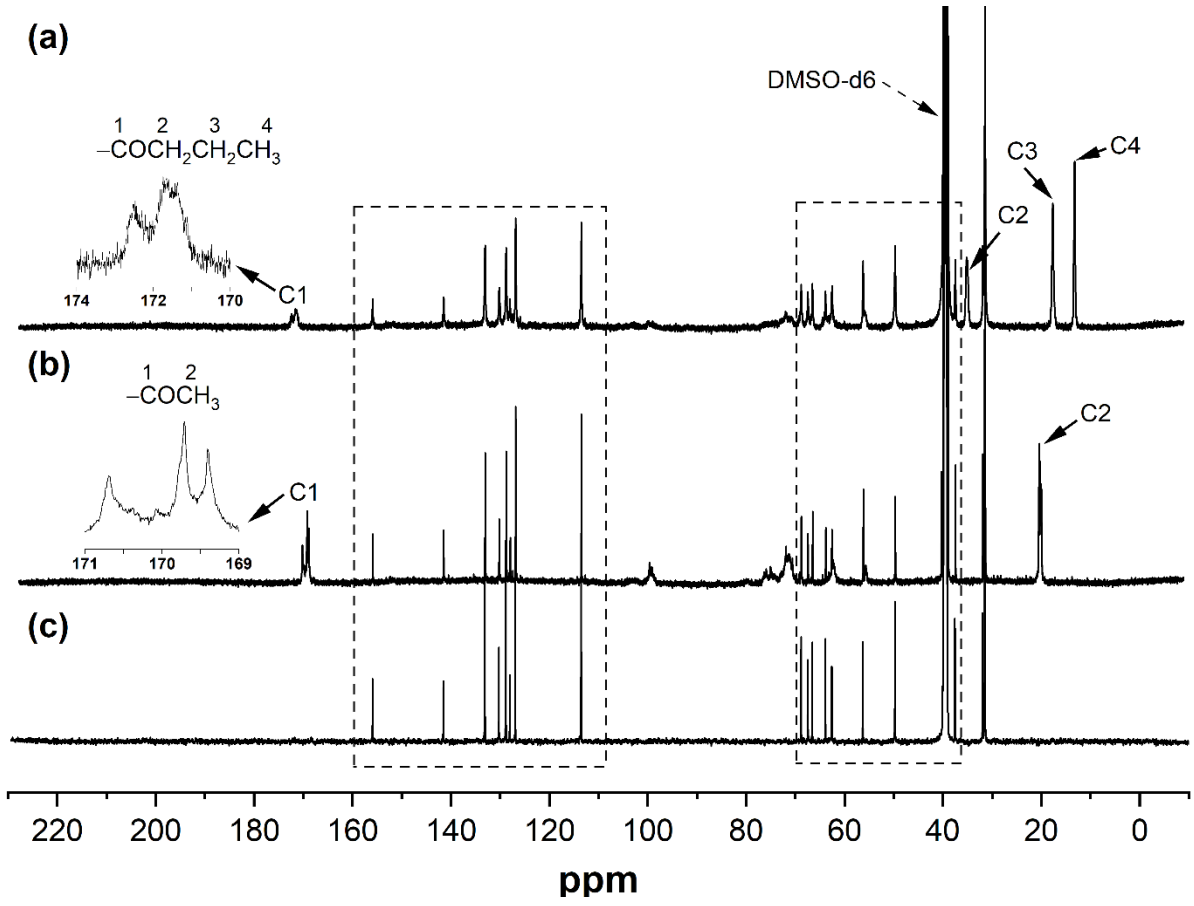

Fig. 1. Solution-state ^{13}C NMR spectra of modified lignocellulose from (a) BA-series (B2, Table 1a), (b) AA-series (A7, Table 1b) and (c) pure hyamine. Rectangular boxes highlight the chemical shifts in the modified samples similar to those found in hyamine.

Understanding the nature of benzethonium and sulfate species present in the lignocellulose ester was considerably clearer by elemental analysis, as given in Fig. 2. As-received lignocellulose had a small but detectable N content, which was considered to be trace contaminants in the supplied material (though consistently present). Compared with the original material, all modified lignocellulose from both BA and AA-series showed a substantial increase in N content that can only be attributed to the benzethonium species at such relatively high values; additionally, the S content of all modified lignocellulose was also significantly increased, which was assigned to the sulfate groups detected by FTIR analysis. The molar ratio (R) of N to S elements was analyzed using the definition of:

$$R = \frac{(N - N_i)/14}{(S - S_i)/32} \qquad (3)$$

where assuming concentrations of the trace N and S unchanged in modified lignocellulose, *N* and *S* in the equation corresponded to the modified lignocellulose while N_i, and S_i corresponded to the original material. The *R* values for the BA-series was 1.01 ± 0.02 and while it was 1.00 ± 0.04 for the AA-series. The molar equivalence of the benzethonium cation to the sulfate group leads the authors to believe their presence was in the form of benzethonium sulfate ($[C_{27}H_{42}NO_2]^+[R\text{-}OSO_3]^-$), where the sulfate was covalently bonded to the lignocellulose (R). Differences in the benzethonium sulfate content of modified lignocellulose based on run conditions are discussed in a later section.

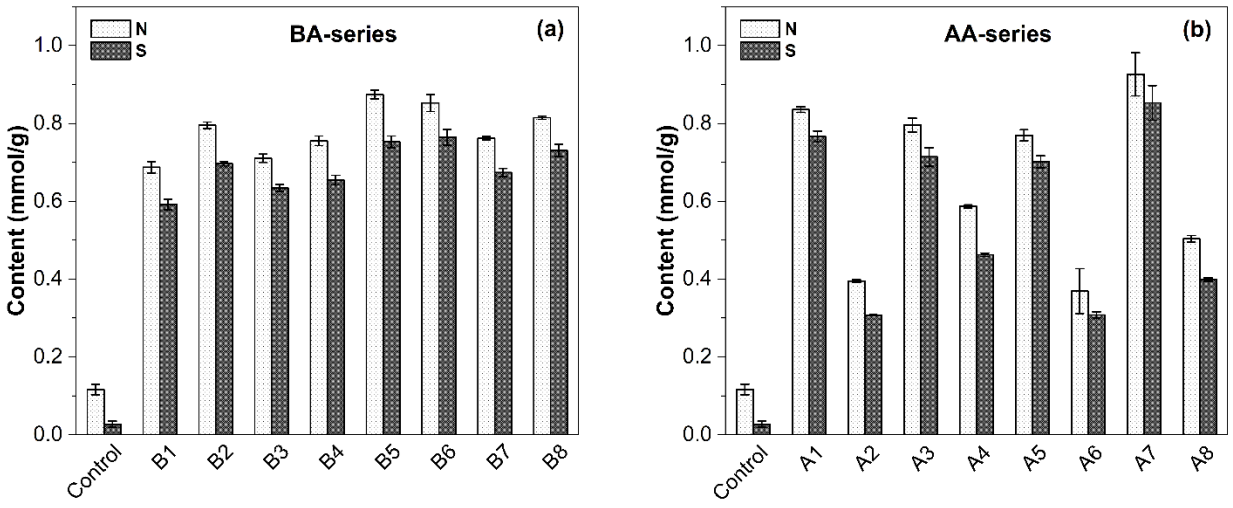

Fig. 2. N and S elemental analysis of the pristine lignocellulose and modified lignocellulose in (a) BA-series and (b) AA-series.

3.2. Thermoplasticity of the modified lignocellulose

After modification by reactive extrusion, all modified lignocellulose displayed distinctive glass transitions, whereas the original lignocellulose had a barely detectable thermal transition. DSC results are presented in supplementary Fig. S3 while detailed analysis of the glass transition by DMA is given below. Correspondingly, all modified lignocellulose in both the BA-series and AA-series displayed flowability during compression molding. Fig. 3 shows that the molded samples of (a) BA-series and (b) AA-series had smooth surfaces and well-defined edges, indicating suitable thermoplasticization of the lignocellulose to flow into all areas of the mold. Molding caused a change in the colour of the modified lignocellulose, going from light brown to uniform black, probably because of thermal oxidation of lignocellulose (Gao, Zhang, & Chang, 2004; Sandoval-Torres, Jomaa, Marc, & Puiggali, 2010), but this was not considered a negative issue since many plastics are coloured black for applications in the automotive or food packaging industries. The molding conditions were probably too long for the biopolymer, but as the

mechanical testing will show, strength was not significantly deteriorated relative to literature-quoted values for cellulose.

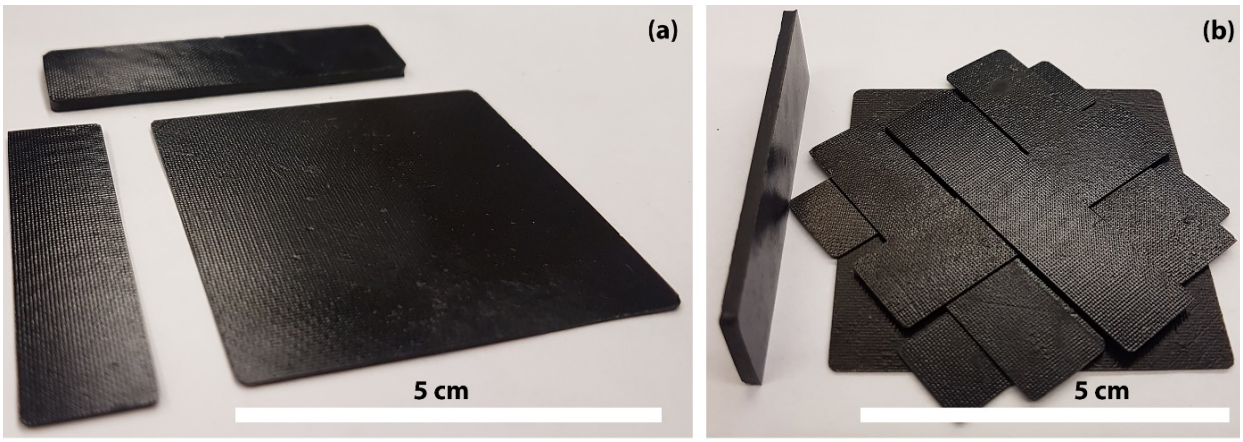

Fig. 3. Images of compression-molded lignocellulose from the (a) BA-series and (b) AA-series, prepared in molds of different dimensions (50 mm × 50 mm × 0.26 mm; 50 mm × 13 mm × 0.45 mm; 55 mm × 15 mm × 2 mm).

Assessing the glass transition temperature (T_g) of the modified lignocelluloses was done by DMA testing. Fig. 3 shows T_g values for the BA-series (Fig. 3a, b) were 72-114 °C while the AA-series (Fig. 3c, d) varied between 119-153 °C, depending on extrusion conditions. All samples in the BA-series were considered to display better thermoplasticity than those in the AA-series based on the T_g. Samples prepared with a 1.2 sulfuric acid/hyamine molar ratio generally had better thermoplasticity (T_g = 72-80 °C) than those based on a 0.95 ratio (T_g = 77-114 °C) in the BA-series. An opposite tendency was observed for AA-series; T_g of samples prepared with a molar ratio of 1.2 versus 0.95 was 135-153 °C versus 119-126 °C. These differences in thermoplasticity among the modified lignocellulose are discussed in a later section.

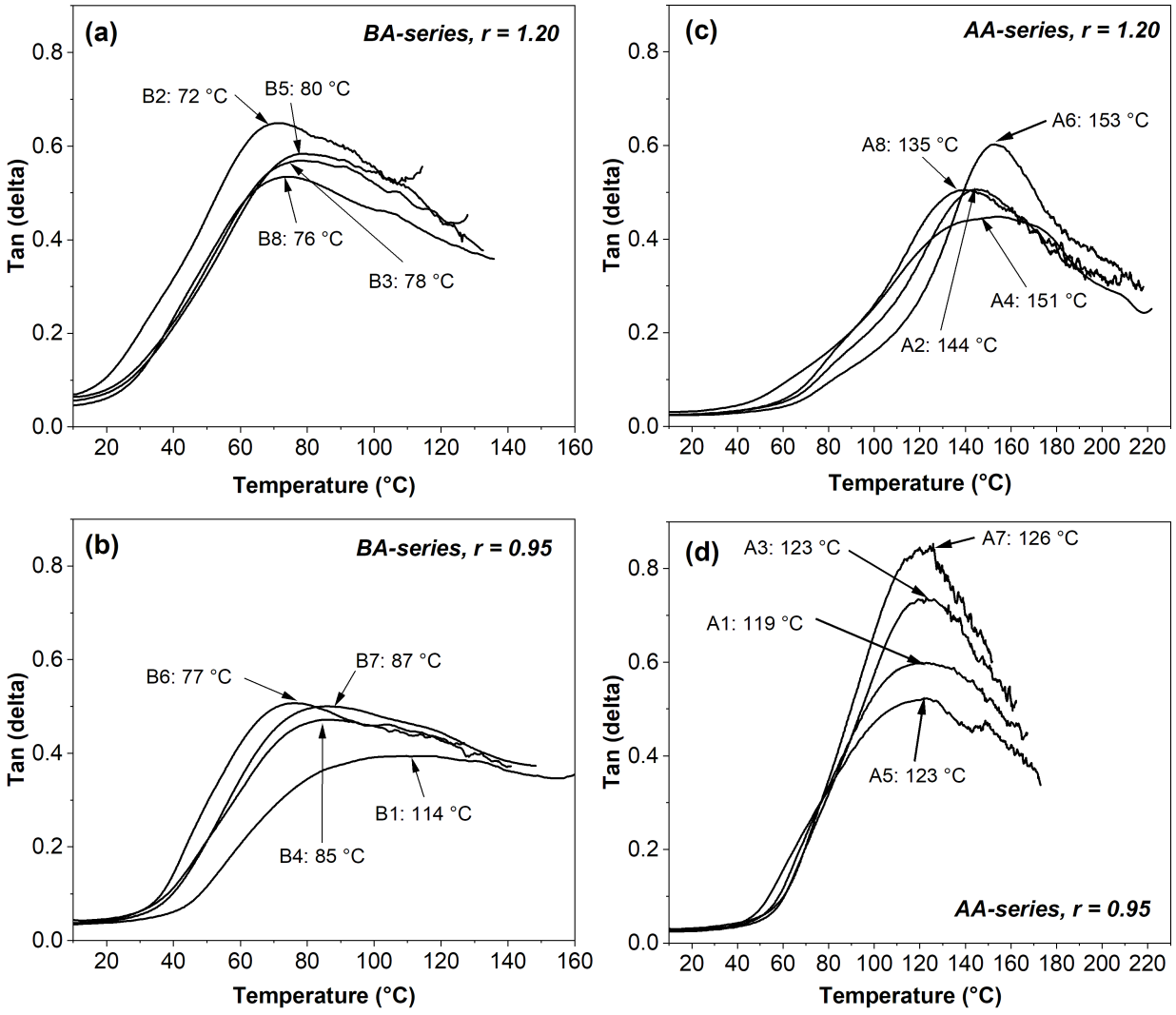

289

290 **Fig. 4.** Loss factor (tan (delta)) of the modified lignocellulose in (a, b) BA-series and (c,d) AA-
291 series determined by DMA testing.

292

293 Dynamic rheological characterization was considered as additional evidence of
294 thermoplasticity for the modified lignocellulose. Fig. 5 shows complex viscosity-temperature
295 curves for the modified lignocellulose in BA-series and AA-series with differing T_g. All samples
296 displayed a significant decrease in viscosity for elevated temperatures above their corresponding
297 T_g. A lower T_g generally corresponded to lower viscosity. The material with the highest T_g = 153

°C from the AA-series showed the weakest decline in viscosity across the range of tested temperatures, giving a more solid-like response above 160 °C. However, even this material showed flowable properties when compression molded, at least when under appropriate pressure, *e.g.,* 6 MPa used in the present study.

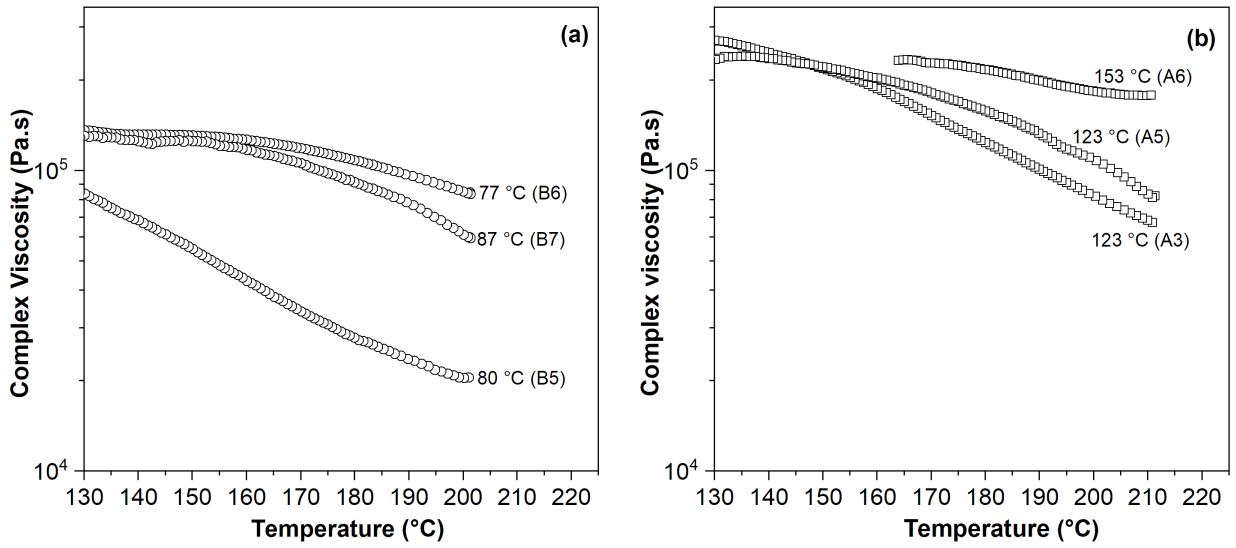

Fig. 5. Comparison of flowability of modified lignocellulose with different T_g in (a) BA-series and (b) AA-series.

3.3. Influence of esterification on the thermoplasticity of modified lignocellulose

Table 2 presents three groupings of thermoplastic lignocellulose from the BA-series and AA-series. The two samples in each group were selected for having similar grafted benzethonium sulfate content and intrinsic viscosity but differed in their acyl content. The table shows that in the three groups, thermoplastics from the AA-series had a degree of acylation nearly double the BA-series, while the samples of the BA-series had lower T_g values. This analysis shows that T_g of the sample was more strongly influenced by the size of the acyl side chains rather than its content. The

313 butyryl group contributed more effectively to matrix mobility than the acetyl group and hence,
314 yielded better thermoplasticity for the modified lignocellulose in BA-series.

315 **Table 2.** Comparison of the degree of modification, intrinsic viscosity and T_g among modified
316 lignocellulose in BA-series and AA-series.

Sample	Acyl (mmol/g)	Sulfate benzethonium (mmol/g)	Intrinsic viscosity (mL/g)	T_g (°C)
B5	1.37 ± 0.01	0.75 ± 0.01	140	80
A1	3.66 ± 0.01	0.75 ± 0.01	158	119
B2	1.62 ± 0.20	0.68 ± 0.01	168	72
A3	4.30 ± 0.03	0.70 ± 0.02	174	123
B7	1.56 ± 0.01	0.66 ± 0.01	171	87
A5	3.75 ± 0.01	0.69 ± 0.01	147	123

317

318 *3.4. Influence of extrusion conditions on the modified lignocellulose of BA-series*

319 DOE analysis was conducted for the BA-series (Fig. 6), considering the influence of four
320 factors listed in Table 1a on T_g (thermoplasticity indicator) and the contents of acyl and
321 benzethonium sulfate (reaction effectiveness). The four main factors all had a statistically positive
322 influence (p-value <0.005) on thermoplasticity. A plot of coefficients of each factor's significance
323 was provided in Fig. S5a. Increasing molar ratio in Fig. 6a was most beneficial for thermoplasticity
324 in the BA-series, since the Tg decreased from 77-114 °C at a molar ratio of 0.95 to 72-78 °C at a
325 molar ratio of 1.20. Liquid injection rate and screw speed had a minor influence relative to molar
326 ratio. Temperature had the least effect on T_g.

Increasing molar ratio had a positive influence (p-value <0.001) on both butyrylation (Fig. 6b) and benzethonium sulfate attachment (Fig. 6d); molar ratio was the dominant factor influencing butyrylation (Fig. S5b), similar to thermoplasticity in Fig. 6a. The increasingly acidic environment present with a higher molar ratio was beneficial to both reactions. Although increasing liquid injection rate had no statistical influence (p-value = 0.27) on butyrylation, it had the highest positive significance on benzethonium sulfate attachment (Fig. S5c). Thereby, increasing liquid injection rate displayed the second-highest positive impact on the thermoplasticity in Fig. 6a. The relevance of injection rate for only benzethonium sulfate attachment was considered to be concentration related; in all cases, butyrylation was done in the presence of an excess of butyric anhydride but clearly more hyamine aided the kinetics for its attachment. Increasing screw speed or temperature could only benefit one of the two reactions but simultaneously decreased another one, *e.g.,* increasing screw speed improved the benzethonium sulfate attachment by 6.4%, but, at the same time, it significantly reduced the butyrylation by 15%. Thus, increasing screw speed or temperature had a much less positive impact on thermoplasticity in Fig. 6a than increasing molar ratio and liquid injection rate.

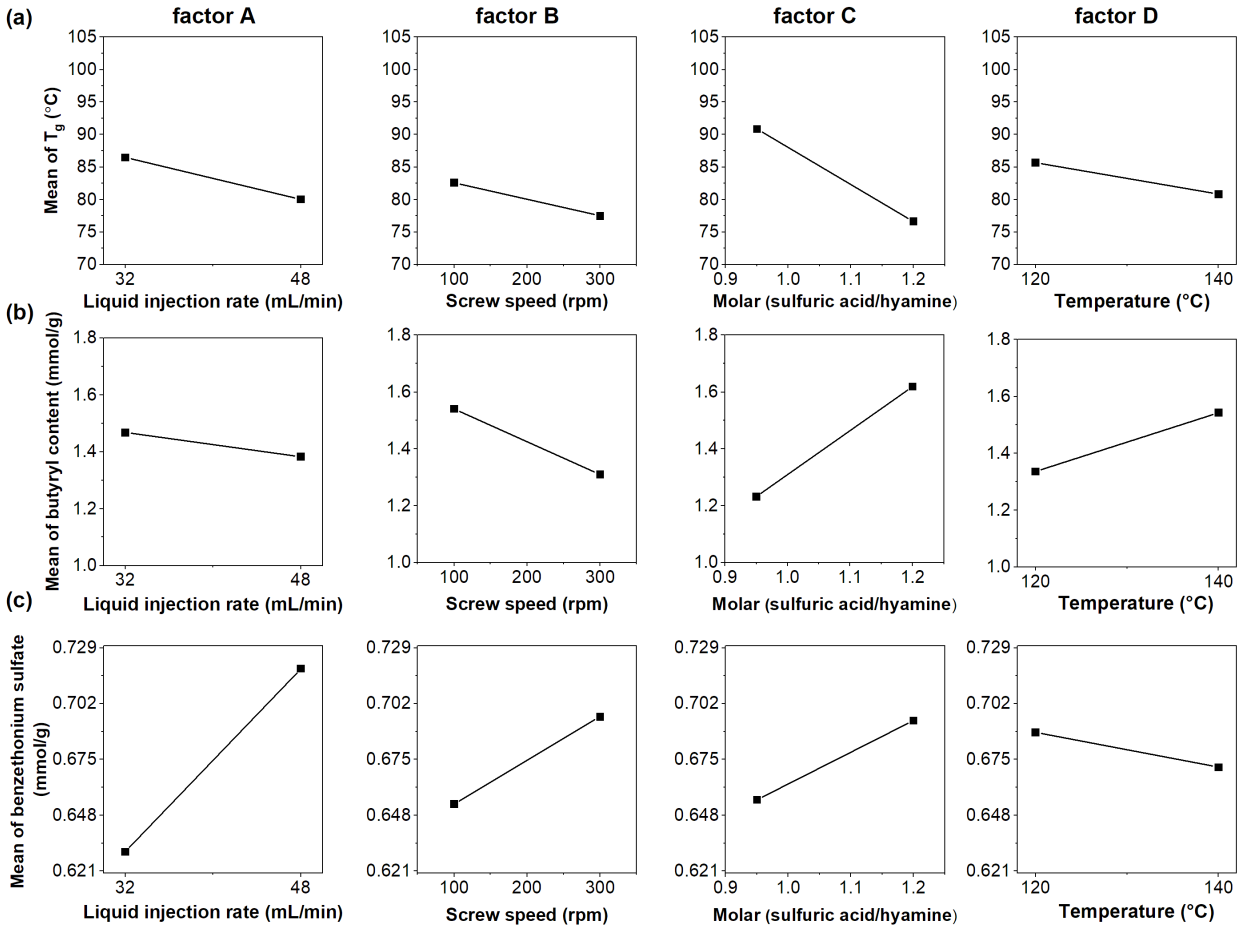

Fig. 6. Main effects plot of the extrusion conditions on (a) T_g, (b) butyryl content and (c) benzethonium sulfate content of modified lignocellulose in BA-series.

3.5. Influence of extrusion conditions on modified lignocellulose of AA-series

DOE analysis of the three main factors listed in Table 1b for AA-series found that increasing molar ratio was the only main factor that significantly (p-value = 0.024) influenced thermoplasticity (Fig. 7a). This was quite different from butyrylation, and so was the fac that increasing molar ratio resulted in higher T_g, indicating inferior thermoplasticity for the AA-series. Correspondingly, increasing molar ratio had a significant influence (p-value < 0.005) on both acetylation and benzethonium sulfate attachment but not necessarily positively. A higher molar ratio increased acetylation (Fig 7b), but simultaneously decreased benzethonium sulfate

attachment (Fig 7c); this influence was not seen with the BA-series suggesting that thermoplasticity was much more reliant on the benzethonium group when acetylation was the chosen modification (which is consistent with benchtop studies (Li et al., 2020)). It was possible the high degree of acetylation (4.2-7.0 mmol/g), as the molar ratio increased from 0.95 to 1.20, consumed hydroxyl functional groups to the detriment of sites for benzethonium sulfate attachment. Butyrylation occurred to a relatively lesser degree (1.6-2.3 mmol/g) and thus, competition for sites with benzethonium sulfate was less of an issue.

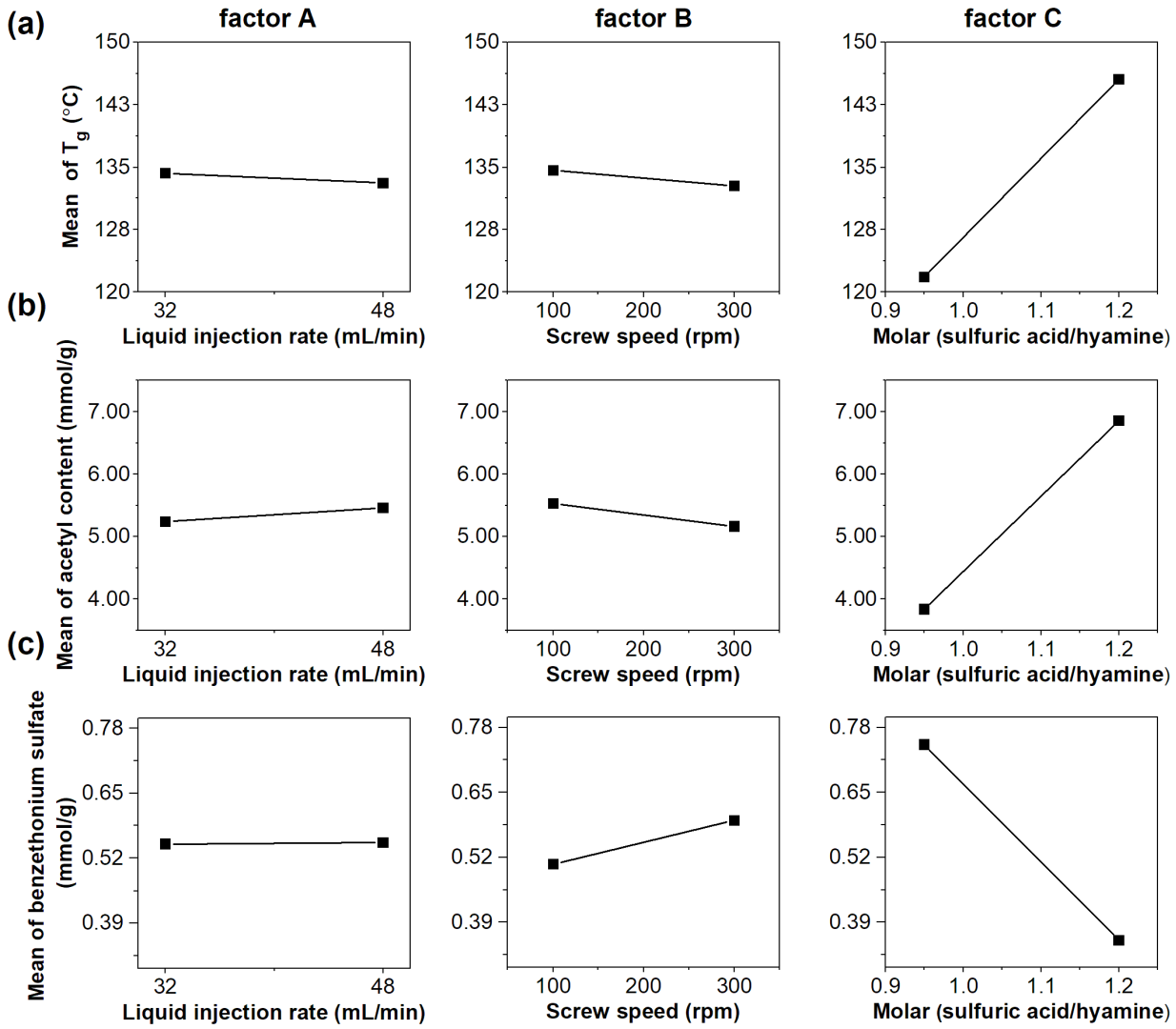

Fig. 7. DOE analysis of the influence of extrusion conditions on (a) T_g, (b) acetyl content and (c) benzethonium sulfate content of modified lignocellulose in AA-series.

3.6. Mechanical properties of thermoplastic lignocellulose

The flexural and tensile moduli of the AA-series were 3.5-5.4 GPa and 1.4-1.8 GPa, respectively, whereas the flexural and tensile moduli of the BA-series were 3.1-4.6 GPa and 1.2-1.6 GPa, respectively. Thermoplastics of AA-series possessed a higher flexural yield strength of 35-46 MPa compared to the BA-series of 23-32 MPa. In comparison, aspen wood pulp has a reported flexural yield strength of 36-68 MPa (Ross, 2010), indicating that the thermoplastic lignocellulose prepared by reactive extrusion was comparable in mechanical strength.

Thermoplastics of the AA-series, with lower T_g, had higher mechanical properties; the sample with the lowest T_g of 119 °C had the highest flexural modulus, flexural strength, and tensile modulus, which were 5.4 GPa, 46 MPa, and 1.8 GPa, respectively. In comparison, thermoplastics in BA-series, with higher T_g, tended to have higher mechanical properties; the sample with the highest T_g of 114 °C had the highest flexural modulus, flexural strength, and tensile modulus, which were 4.6 GPa, 32 MPa, and 1.6 GPa, respectively. The trend for thermoplastics of the BA-series was attributed to chain mobility of a more or less homogenous specimen; it was a reflection of the excellent thermoplasticity of this modified species. Conversely, the modified lignocellulose of the AA-series did not melt entirely as the specimens were molded (Fig. S7b). As a result, the heterogeneity in the molded specimens was felt to be causing this atypical behavior. Only the modified lignocellulose in AA-series with lower T_g temperature formed dense (i.e. non-porous) molded specimens, necessary to display the best mechanical properties.

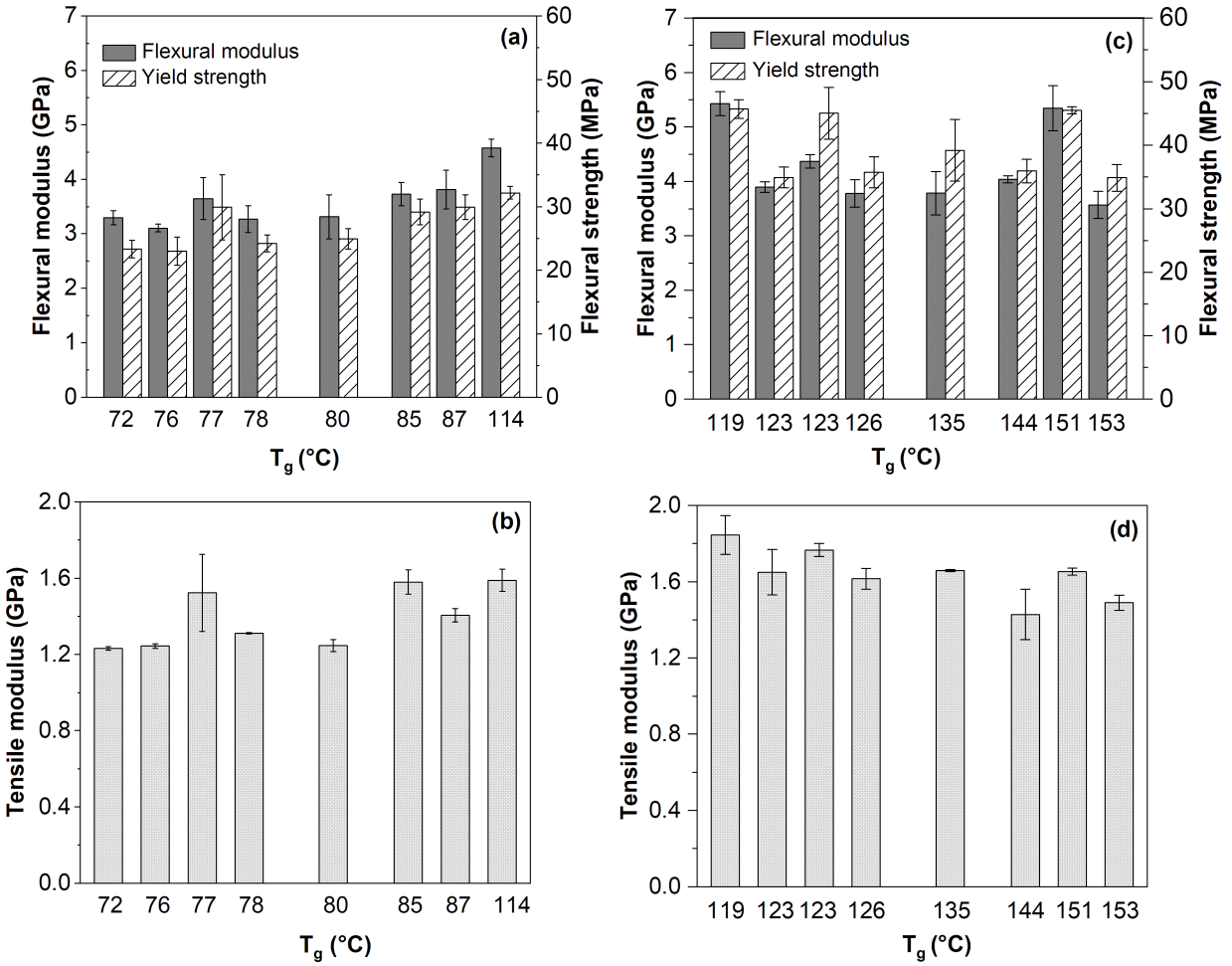

Fig. 8. Flexural and tensile properties of the thermoplastics in **(a, b)** BA-series and (c,d) AA-series.

4. CONCLUSIONS

Despite the short residence time in the extruder, modification of lignocellulose by grafting acyl and benzethonium sulfate was achieved by a new solvent-free reactive extrusion method. The modifications took place to an acceptable degree to afford sufficient thermoplasticity for compression molding. The butyric anhydride-based modifier was superior to acetic anhydride-based modifier in terms of thermoplasticization of lignocellulose relative to the degree of acyl group attachment. A DOE analysis revealed that the molar ratio of sulfuric acid to hyamine, as the novel functionalizing agent in the modification, was the dominant factor to impact the

thermoplasticity of modified lignocellulose in both BA and AA-series. In addition to displaying good moldability, the modified samples showed excellent retention of the original wood pulp's high mechanical properties.

5. Declaration of Competing Interest

The authors associated with McMaster University declare no conflict of interest. David J. W. Lawton is an employee of the Xerox Research Centre of Canada, a division of Xerox Canada.

6. ACKNOWLEDGEMENTS

This research was funded under the Ontario Research Fund (ORF) grant (#07-41) led by Dr. Sain at the University of Toronto. The authors are also grateful to Paul Gatt at McMaster University for making the compression molds, and Dr. Zhicheng Pan at McMaster University for his technical help on the nitrogen and sulfur elemental analysis.

Appendix A. Supplementary data

This article has supplementary material.

7. REFERENCES

Abe, M., Enomoto, Y., Seki, M., & Miki, T. (2020). Esterification of solid wood for plastic forming. *BioResources*, *15*(3), 6282–6298. https://doi.org/10.15376/biores.8.3.6282-6298

Baati, R., Mabrouk, A. Ben, Magnin, A., & Boufi, S. (2018). CNFs from twin screw extrusion and high pressure homogenization: A comparative study. *Carbohydrate Polymers*, *195*, 321–328. https://doi.org/10.1016/j.carbpol.2018.04.104

Baati, R., Magnin, A., & Boufi, S. (2017). High Solid Content Production of Nanofibrillar Cellulose via Continuous Extrusion. *ACS Sustainable Chemistry and Engineering*, *5*(3),

414 2350–2359. https://doi.org/10.1021/acssuschemeng.6b02673

415 Bao, L., Zou, X., Chi, S., Dong, S., Lei, J., & Wang, J. (2018). Advanced sustainable
416 thermoplastics based on wood residue using interface nanomodification technique.
417 *Advanced Sustainable Systems*, *2*(7), 1800050. https://doi.org/10.1002/adsu.201800050

418 Bhandari, P. N., Jones, D. D., & Hanna, M. A. (2012). Carboxymethylation of cellulose using
419 reactive extrusion. *Carbohydrate Polymers*, *87*(3), 2246–2254.
420 https://doi.org/10.1016/j.carbpol.2011.10.056

421 Böke, H., Akkurt, S., Özdemir, S., Göktürk, E. H., & Caner Saltik, E. N. (2004). Quantification
422 of CaCO3-CaSO3·0.5H2O-CaSO4·2H2O mixtures by FTIR analysis and its ANN model.
423 *Materials Letters*, *58*(5), 723–726. https://doi.org/10.1016/j.matlet.2003.07.008

424 Chen, G., Zhang, B., Zhao, J., & Chen, H. (2013). Improved process for the production of
425 cellulose sulfate using sulfuric acid/ethanol solution. *Carbohydrate Polymers*, *95*(1), 332–
426 337. https://doi.org/10.1016/j.carbpol.2013.03.003

427 Chen, J., Tang, C., Yue, Y., Qiao, W., Hong, J., Kitaoka, T., & Yang, Z. (2017). Highly
428 translucent all wood plastics via heterogeneous esterification in ionic liquid/dimethyl
429 sulfoxide. *Industrial Crops and Products*, *108*(June), 286–294.
430 https://doi.org/10.1016/j.indcrop.2017.06.054

431 Chen, J., Yu, Y., Han, J., Guo, Y., Yang, Z., Shang, Q., & Liu, C. (2019). Mechanochemical
432 esterification of waste mulberry wood by wet Ball-milling with tetrabutylammonium
433 fluoride. *Bioresource Technology*, *285*, 121354.
434 https://doi.org/10.1016/j.biortech.2019.121354

435 Chen, M., & Shi, Q. (2015). Transforming sugarcane bagasse into bioplastics via homogeneous

436 modification with phthalic anhydride in ionic liquid. *ACS Sustainable Chemistry &*
437 *Engineering*, *3*(10), 2510–2515. https://doi.org/10.1021/acssuschemeng.5b00685

438 Correia, V. da C., dos Santos, V., Sain, M., Santos, S. F., Leão, A. L., & Savastano Junior, H.
439 (2016). Grinding process for the production of nanofibrillated cellulose based on
440 unbleached and bleached bamboo organosolv pulp. *Cellulose*, *23*(5), 2971–2987.
441 https://doi.org/10.1007/s10570-016-0996-9

442 Darwish, S., Wang, S.-Q., Croker, D. M., Walker, G. M., & Zaworotko, M. J. (2019).
443 Comparison of mechanochemistry vs solution methods for synthesis of 4,4′-bipyridine-
444 basedcoordination polymers. *ACS Sustainable Chemistry & Engineering*, *7*(24), 19505–
445 19512. https://doi.org/10.1021/acssuschemeng.9b04552

446 Espinosa, E., Rol, F., Bras, J., & Rodríguez, A. (2019). Production of lignocellulose nanofibers
447 from wheat straw by different fibrillation methods. Comparison of its viability in cardboard
448 recycling process. *Journal of Cleaner Production*, *239*, 118083.
449 https://doi.org/10.1016/j.jclepro.2019.118083

450 Feng, Y., Cheng, H., Lei, B., Liang, Y., Yang, Z., & Hezhi, H. (2019). Towards sustainable
451 thermoplastic woody materials prepared from continuous steam explosion followed by
452 oxidation-reduction. *Carbohydrate Polymers*, *216*, 322–330.
453 https://doi.org/10.1016/j.carbpol.2019.04.019

454 Gan, T., Zhang, Y., Chen, Y., Hu, H., Yang, M., Huang, Z., … Huang, A. (2018). Reactivity of
455 main components and substituent distribution in esterified sugarcane bagasse prepared by
456 effective solid phase reaction. *Carbohydrate Polymers*, *181*, 633–641.
457 https://doi.org/10.1016/j.carbpol.2017.11.102

458 Gao, J., Zhang, B., & Chang, J. (2004). Induced discoloration of buerger maple during drying
459 process. *Forestry Studies in China*, *6*(2), 50–55. https://doi.org/10.1007/s11632-004-0020-6

460 Guo, Y., Chen, J.-Q., Su, M., & Hong, J.-G. (2018). Bio-based plastics with highly efficient
461 esterification of lignocellulosic biomass in 1-methylimidazole under mild conditions.
462 *Journal of Wood Chemistry and Technology*, *38*(4), 338–349.
463 https://doi.org/10.1080/02773813.2018.1488876

464 Ho, T. T. T., Abe, K., Zimmermann, T., & Yano, H. (2015). Nanofibrillation of pulp fibers by
465 twin-screw extrusion. *Cellulose*, *22*(1), 421–433. https://doi.org/10.1007/s10570-014-0518-
466 6

467 Hoeger, I. C., Nair, S. S., Ragauskas, A. J., Deng, Y., Rojas, O. J., & Zhu, J. Y. (2013).
468 Mechanical deconstruction of lignocellulose cell walls and their enzymatic saccharification.
469 *Cellulose*, *20*(2), 807–818. https://doi.org/10.1007/s10570-013-9867-9

470 Howard, J. L., Cao, Q., & Browne, D. L. (2018). Mechanochemistry as an emerging tool for
471 molecular synthesis: what can it offer? *Chemical Science*, *9*(12), 3080–3094.
472 https://doi.org/10.1039/C7SC05371A

473 Huang, K., Wang, B., Cao, Y., Li, H., Wang, J., Lin, W., … Liao, D. (2011). Homogeneous
474 preparation of cellulose acetate propionate (CAP) and cellulose acetate butyrate (CAB)
475 from sugarcane bagasse cellulose in ionic liquid. *Journal of Agricultural and Food*
476 *Chemistry*, *59*(10), 5376–5381. https://doi.org/10.1021/jf104881f

477 Huang, L., Wu, Q., Wang, Q., Ou, R., & Wolcott, M. (2020). Solvent-free pulverization and
478 surface fatty acylation of pulp fiber for property-enhanced cellulose/polypropylene
479 composites. *Journal of Cleaner Production*, *244*, 118811.

https://doi.org/10.1016/j.jclepro.2019.118811

Huang, L., Wu, Q., Wang, Q., & Wolcott, M. (2019). One-step activation and surface fatty acylation of cellulose fibers in a solvent-free condition. *ACS Sustainable Chemistry & Engineering*, *7*(19), 15920–15927. https://doi.org/10.1021/acssuschemeng.9b01974

Jiang, J., Wang, J., Zhang, X., & Wolcott, M. (2017). Microstructure change in wood cell wall fracture from mechanical pretreatment and its influence on enzymatic hydrolysis. *Industrial Crops and Products*, *97*, 498–508. https://doi.org/10.1016/j.indcrop.2017.01.001

Kono, H., Oka, C., Kishimoto, R., & Fujita, S. (2017). NMR characterization of cellulose acetate: Mole fraction of monomers in cellulose acetate determined from carbonyl carbon resonances. *Carbohydrate Polymers*, *170*, 23–32. https://doi.org/10.1016/j.carbpol.2017.04.061

Li, J., Thompson, M., & Lawton, D. J. W. (2019). Improved chemical reactivity of lignocellulose from high solids content micro-fibrillation by twin-screw extrusion. *Journal of Polymers and the Environment*, *27*(3), 643–651. https://doi.org/10.1007/s10924-019-01377-3

Li, J., Zhang, H., Sacripante, G. G., Lawton, D. J. W., Marway, H. S., & Thompson, M. R. (2020). Solvent-free modification of lignocellulosic wood pulp into a melt-flowable thermoplastic. *Cellulose*. https://doi.org/10.1007/s10570-020-03589-6

Ochiai, B., Watanabe, T., Hanzawa, C., Akiyama, K., Matsumura, Y., Shimura, R., … Nishioka, A. (2019). Milling in Seconds Accelerates Acetylation of Cellulose in Hours. *ACS Omega*, *4*(17), 17542–17546. https://doi.org/10.1021/acsomega.9b02422

Ralph, J., & Landucci, L. (2010). NMR of Lignins. In *Lignin and Lignans* (pp. 137–243). CRC Press. https://doi.org/10.1201/EBK1574444865-c5

Rol, F., Karakashov, B., Nechyporchuk, O., Terrien, M., Meyer, V., Dufresne, A., … Bras, J. (2017). Pilot-Scale Twin Screw Extrusion and Chemical Pretreatment as an Energy-Efficient Method for the Production of Nanofibrillated Cellulose at High Solid Content. *ACS Sustainable Chemistry & Engineering*, *5*(8), 6524–6531. https://doi.org/10.1021/acssuschemeng.7b00630

Ross, R. J. (2010). *Wood handbook : wood as an engineering material*. https://doi.org/10.2737/FPL-GTR-190

Sandoval-Torres, S., Jomaa, W., Marc, F., & Puiggali, J.-R. (2010). Causes of color changes in wood during drying. *Forestry Studies in China*, *12*(4), 167–175. https://doi.org/10.1007/s11632-010-0404-8

Vaidya, A. A., Gaugler, M., & Smith, D. A. (2016). Green route to modification of wood waste , cellulose and hemicellulose using reactive extrusion. *Carbohydrate Polymers*, *136*, 1238–1250. https://doi.org/10.1016/j.carbpol.2015.10.033

Xie, H., King, A., Kilpelainen, I., Granstrom, M., & Argyropoulos, D. S. (2007). Thorough chemical modification of wood-based lignocellulosic materials in ionic liquids. *Biomacromolecules*, *8*(12), 3740–3748. https://doi.org/10.1021/bm700679s

Zhang, Q., Zhang, X., Zhu, Z., Zhang, A., Zhang, C., Wang, X., & Liu, C. (2018). Mechanocatalytic Solvent-Free Esterification of Sugarcane Bagasse. *Polymers*, *10*(3), 282. https://doi.org/10.3390/polym10030282

Zhang, Y., Li, H., Li, X., Gibril, M. E., & Yu, M. (2014). Chemical modification of cellulose by in situ reactive extrusion in ionic liquid. *Carbohydrate Polymers*, *99*, 126–131. https://doi.org/10.1016/j.carbpol.2013.07.084

524 Zhen, L., Zhang, G., Huang, K., Ren, X., Li, R., & Huang, D. (2016). Modification of rice straw
525 for good thermoplasticity via graft copolymerization of ε-caprolactone onto acetylated rice
526 straw using ultrasonic-microwave coassisted technology. *ACS Sustainable Chemistry &*
527 *Engineering*, *4*(3), 957–964. https://doi.org/10.1021/acssuschemeng.5b01039

528

529